AUT Journal of Civil Engineering

AUT J. Civil Eng., 6(1) (2022) 119-132
DOI: 10.22060/ajce.2022.20915.5785

Three-Dimensional Numerical Study of the Tensile Capacity of Helical Multi-Plates Anchors

M.Hazeghian* , M. Abdoli, A. R. Javid

Department of Civil Engineering, Yazd University, Yazd, Iran.

ABSTRACT: Nowadays, helical anchors are one of the fastest methods of supporting excavations. The use of helical anchors is increasing, and recently they received more attention in researches. One of the most important factors for the design of helical anchors is their tensile capacity, to which less attention was paid in the literature compared with the helical piles. The present study uses a three-dimensional numerical modeling approach to investigate the tensile capacity of helical multi-plate anchors. For this purpose, first, the adopted numerical modeling methodology is verified. Then, a comprehensive parametric study is performed to investigate the effects of various parameters involving the soil type, soil cohesion, plate diameter, plate spacing, surcharge, and anchor inclination. The present study results show that the tensile capacities of the helical multi-plate anchors increase by increasing the plate's diameter, surcharge, and soil relative density. However, the soil cohesion and anchor inclination have negligible effects. Moreover, the results indicate that the load-bearing shares of the shaft increase by increasing the surcharge and decreasing the plate diameter. In addition, the results show that the load-bearing shares of the plates stay about constant for S/D≥4 (S and D represent the plate's Spacing and Diameter, respectively). So that the failure mechanism of multi-plate anchors could be considered as the individual plate for S/D≥4 and cylindrical shear for S/D<4. In other words, the critical S/D ratio is 4. The union of failure zones formed around the plates in displacement contours for S/D<4 confirms this result.

Review History:

Received: Dec. 25, 2021
Revised: Jul. 15, 2022
Accepted: Jul. 20, 2022
Available Online: Jul. 30, 2022

Keywords:

Helical multi-plates anchors
Flac3D
Three-dimensional numerical study
Tensile capacity
Load-bearing shares of plates

1- Introduction

The earliest usage of helical elements (i.e., screw elements) for the foundation of a lighthouse was reported by the civil engineer Alexander Mitchell in 1833 [1]. Nowadays, the applications of helical elements have extended significantly. They are used as helical piles, helical micro piles, helical nails, and anchors. The focus of the present paper is on helical anchors, which are now used as one of the main methods for supporting excavations. Based on Clemence and lutenegger [2], the usage of helical anchors as the excavation support could be considered as the third application of helical elements. The design standards for helical anchors have increased remarkably in the last decades.

A lot of experimental [1, 3-19] and numerical [20-35] researches have been reported about helical elements. Some of them would be explained briefly in the following.

Kwon, Lee, Kim, Kim and Lee [23] conducted a numerical study on the ultimate capacity of helical piles subjected to inclined loads in saturated clays. They showed that the ultimate capacity of helical piles decreases considerably by increasing the load inclination concerning vertical. Moreover, Kwon, Lee, Kim, Kim, and Lee [23] concluded that the ultimate capacity of helical anchors in the case that the diameters of plates are increasing from top to bottom is comparatively higher than in the case that they are decreasing.

*Corresponding author's email: m.hazeghian@yazd.ac.ir

An experimental study on the uplift capacity of helical monopiles in dense and loose sands was done by Nazir, Chuan, Niroumand, and Kassim [1]. This study indicated that the failure zone formed around the helical pile in dense sand is more extensive than that of loose sand. Moreover, Nazir, Chuan, Niroumand, and Kassim [1] developed experimental equations to evaluate the uplift capacity of helical piles. They showed that these equations are in agreement with the previous studies.

Rawat and Gupta [27] conducted a comprehensive two-dimensional numerical study on the performance of tensile multi-plate helical piles. In their study, the critical spacing between helical plates was obtained three times the diameter of the plates. In other words, they showed that if the spacing of the plates is higher than three times their diameter, the individual plate failure mechanism occurs; otherwise, the cylindrical shear failure mechanism takes place.

The performance of helical and grouted nails subjected to pullout forces was compared in an experimental study by Tokhi, Ren, and Li [18] They showed that the increasing effect of surcharge on the pullout capacity of helical nails compared with grouted nails is higher. Moreover, they resulted in the displacements required to mobilize the pullout capacity of helical and grouted nails being almost the same. In total, the results of this study showed that the performance of helical nails subjected to tensile loadings is much better than grouted nails.

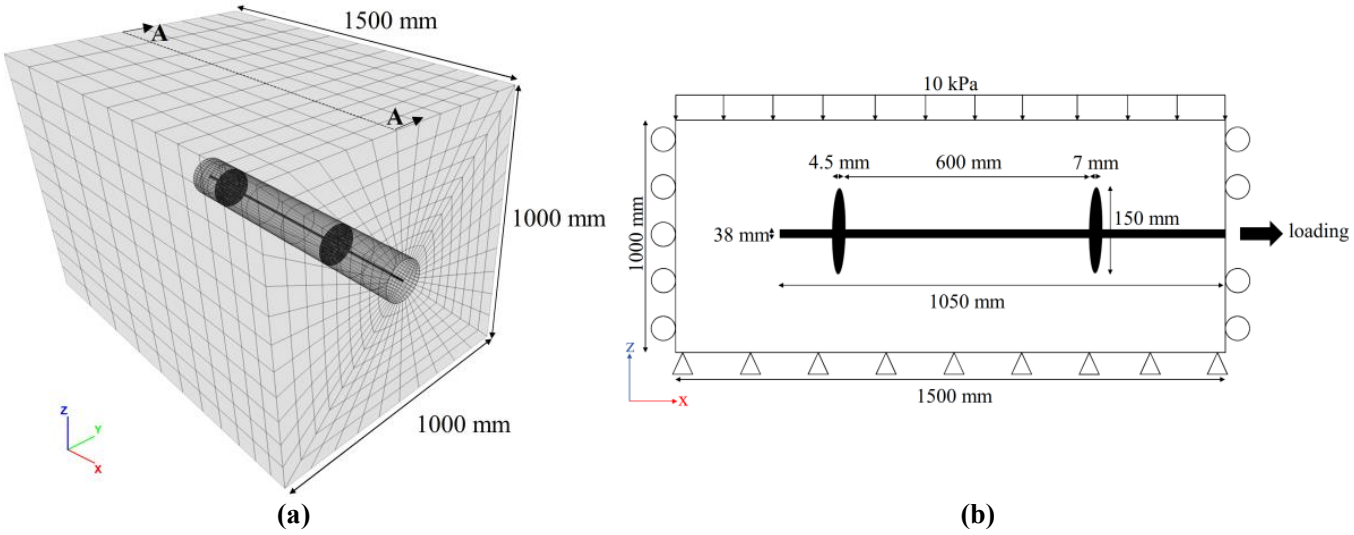

Fig. 1. Model geometry: a) 3D model, b) Section A-A.

Most of the previous studies about helical elements focused on helical piles. However, the helical anchors were less taken into account. The present paper adopts a three-dimensional numerical methodology to investigate the tensile capacity of multi-plate helical anchors (2-plates and 3-plates anchors). In the present paper, first, the employed numerical modeling methodology is verified by a pullout test experiment. Then, a comprehensive parametric study is performed to investigate the effects of various parameters involving the soil type, soil cohesion, surcharge, anchor inclination, plate diameter, and spacing. Then, the numerical tensile capacities are compared with the analytical ones. Moreover, the present paper studies the load-bearing shares of the shaft and helical plates, to which less attention was paid in the previous studies. The load-bearing shares of the plates could be used to determine the critical plate spacing of multi-plate anchors.

2- Verification

FLAC 3D software was employed to perform numerical simulations of the present study. To verify the software and numerical simulation procedure, an experimental pullout test carried out by Tokhi, Ren, and Li [18] was modeled. Fig. 1 shows the numerical model, boundary conditions, and mesh structure. The geometry of the test box and helical anchor, as well as the surcharge, were assumed the same as in the experiment. As indicated in Fig. 1, the bottom of the model was assumed to be fixed in both directions but its lateral boundaries were fixed only in the normal direction.

The constitutive model of the soil was assumed Mohr-Coulomb. Moreover, Elastic cable and liner structural elements [36] were employed for the shaft and helical plates, respectively. The interaction parameters between soil and structure elements were determined based on the FLAC 3D manual [36]. Table 1 summarizes the properties of the soil, shaft, and helical plate.

The numerical modeling methodology for the pull-out tests is as follows: first, initial stresses under gravity were applied in the model. Then, the 10 kPa surcharge was imposed on the top of the soil block. After the equilibrium was obtained, the helical anchor was pulled out gradually through several loading steps. In each step, 1kN force was applied to the head of the anchor, and it allowed the model to reach equilibrium. The loading steps were repeated until the helical anchor failed (i.e., the force-displacement curve became almost asymptotic).

Table 1. Properties of the soil, shaft, and helical plates [18].

Soil	Density (ρ)	1.74 t/m^3
	Modulus of elasticity (E)	50 MPa
	Poisson's ratio (v)	0.30
	Friction angle (φ)	33.60^o
	Cohesion (c)	0
Shaft	Young Modulus (E_s)	200 GPa
	Relative stiffness (k_s)	6.25 MN/m^2
	Skin friction angle (φ_s)	2/3φ
	Skin cohesion (c_s)	2/3c
	Perimeter (p_s)	0.12 m
Plates	Young Modulus (E_p)	200 GPa
	Poisson's ratio (v_p)	0.25
	Relative normal stiffness (k_{np})	1.0 GN/m^3
	Relative shear stiffness (k_{sp})	1.0 GN/m^3
	Skin friction angle (φ_p)	2/3φ
	Skin cohesion (c_p)	2/3c

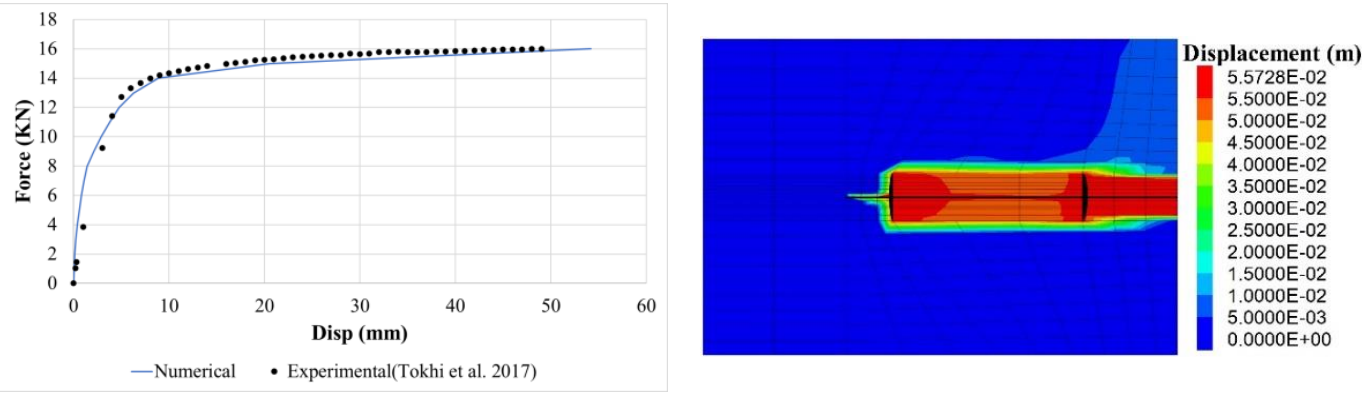

a b

Fig. 2. a) Comparison of the experimental and numerical force-displacement curves, b) Contour of displacement magnitude at the end of the test.

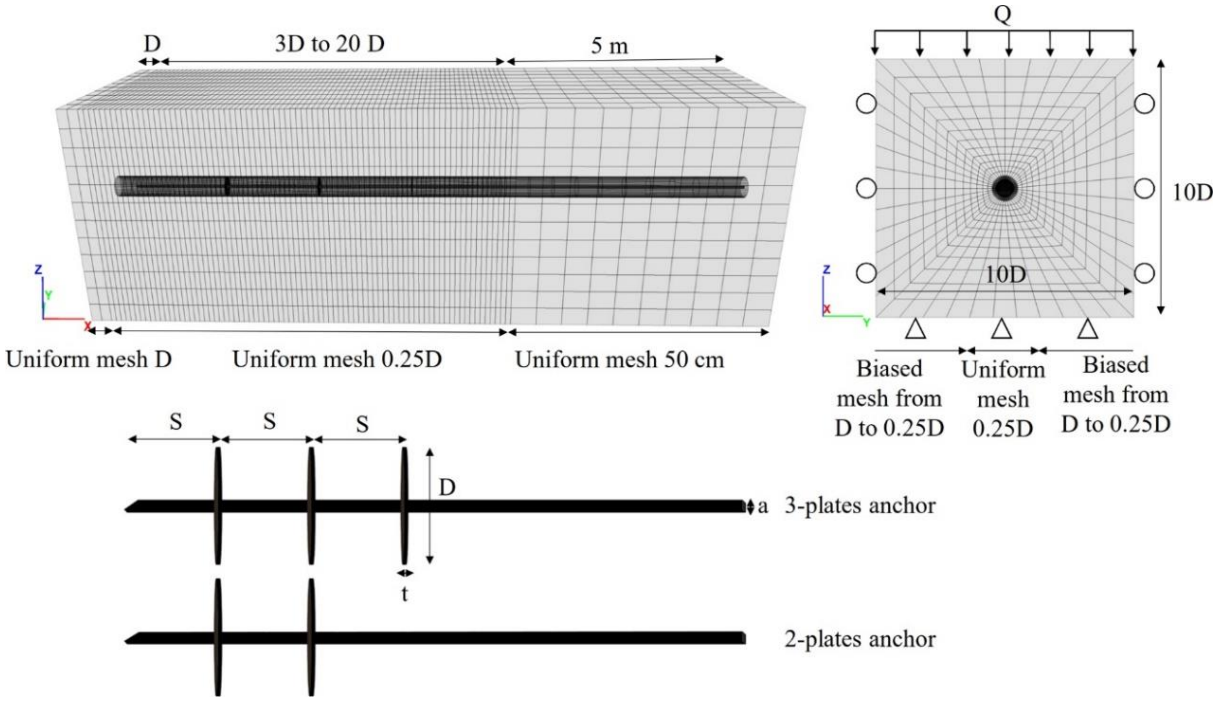

Fig. 3. Geometry, dimensions, and mesh structure of the numerical model used in the parametric study.

Fig. 2 (a) compares the numerical and experimental force-displacement curves. As can be seen, they are almost matched during loading. In addition, Fig. 2 (b) shows the contour of displacement magnitude at the end of the test. It can be seen that a shallow failure occurs for the helical anchor because its first plate (i.e., top plate) locates near the soil block front surface. In this failure mechanism, a soil cylinder around the helical anchor extending from its second plate (i.e., bottom plate) to the soil block front surface is sheared. Therefore, the helical anchor and this soil cylinder pull out simultaneously.

3- Problem Description

A parametric study involving 58 three-dimensional analyses was carried out to investigate the tensile capacity of multi-plate helical anchors (i.e., 2-plate and 3-plate helical anchors). The effect of the soil type, soil cohesion (c), surcharge (Q), plate diameter (D), plate spacing (S), and anchor inclination (θ) on the tensile capacity of multi-plate helical anchors were investigated. Moreover, the present paper studies the load-bearing shares of the helical plates and shaft, to which less attention was paid in previous studies.

Fig. 3 illustrates the geometry, dimensions, and mesh structure of the 3-D model employed in the parametric study. The model dimensions were selected based on the study of Kwon, Lee, Kim, Kim, and Lee [23] to minimize the effect of boundary conditions. The free length of the shaft (i.e., the distance between the first plate and the soil block front surface) was assumed 5m. Moreover, the distance between the

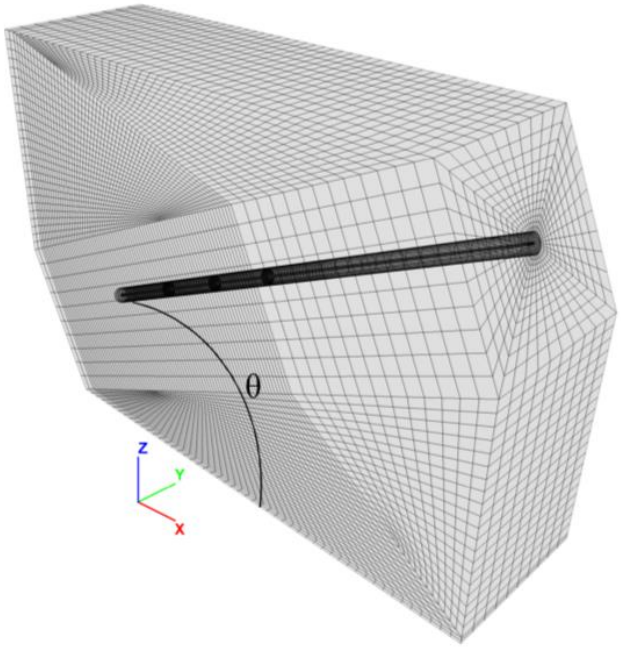

Fig. 4. Numerical model used for a θ=25° inclined anchor.

end of the shaft and the soil block back surface was assumed to be equal to the plate's diameter, D. The boundary conditions are similar to Fig. 1 (b). A different geometry was used for inclined anchors; Fig. 4 shows the numerical model for a θ=25° inclined anchor.

Five types of soil were used in the parametric study. These soils were numbered from 1 (very loose) to 5 (very dense). The properties of the soil types are given in Table 2.Table 3 indicates the range of variation of parameters in the parametric study. The parameters for the 2-plate and 3-plate **reference models** are bold and underlined. According to the Chance standard [37], the size of the shaft (a) and the thickness of the plates (t) were assumed a = 57 mm and t = 13 mm for D = 50-60 cm, respectively and a = 73 mm and t = 19 mm for D = 20-40 cm, respectively.

4- Results and Discussion

Fig. 7 shows the variation of tensile capacities versus various parameters involving the soil type (1-5), surcharge (Q), soil cohesion (c), plate's diameter (D), plate spacing in terms of Spacing to Diameter (S/D) ratio and anchor inclination (θ). As can be seen, the tensile capacities of multi-plate anchors increase remarkably by increasing the soil density, surcharge, and plate diameter. It is noteworthy that the increasing rate of tensile capacities versus the plate's diameter is considerably higher for D>40 cm. From an engineering point of view, it can be seen that the tensile capacities remain approximately unchanged by the increase of soil cohesion. In addition, Fig. 7 shows that the tensile capacities stay almost constant by increasing the anchor inclination. As far as the plate spacing is concerned, it can be seen that the tensile capacities increase considerably up to S/D=4 and then remain unaltered. This can be attributed to the transition of the failure mechanism from cylinder shear to the individual plate [21, 23, 27, 37], which will be discussed later in Section 4.3.

Table 2. Properties of the soil types used in the parametric study.

Soil type	1=Very loose	2=Loose	3=Medium	4=Dense	5=Very dense
Relative density, Dr (%)	15	35	65	85	100
Void ratio (e)	0.84	0.76	0.64	0.56	0.5
γ (kN/m^3)	15.5	16.2	17.4	18.3	19.0
E (MPa)	10	25	50	65	80
φ^o	28	30	36	41	45
$\psi^o=\varphi^o$-30^o	0	0	6	11	15

Table 3. The range of parameters in the parametric study.

Soil type (Table 2)	c (kPa)	Q (kPa)	D (cm)	S/D	θ^o
				1	
1	0	100	20	2	**0**
2	5	150	30	3	5
3	**10**	**200**	**40**	4	10
4	15	250	50	**5**	15
5	20	300	60	6	20
				7	25
				8	

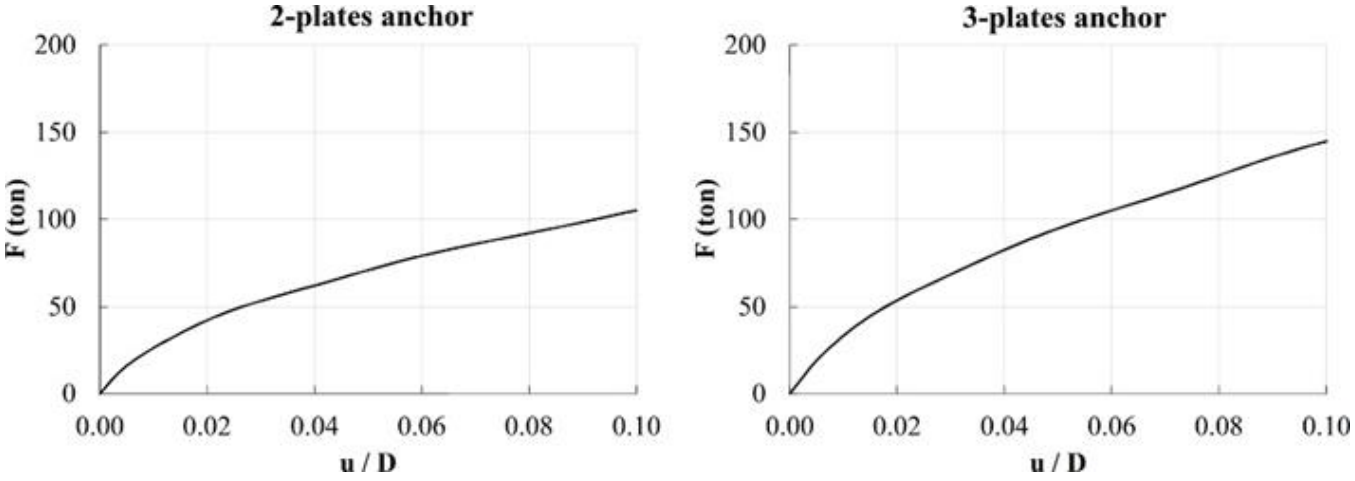

Fig. 5. Force versus normalized net displacement curves of the 2-plate and 3-plate reference models.

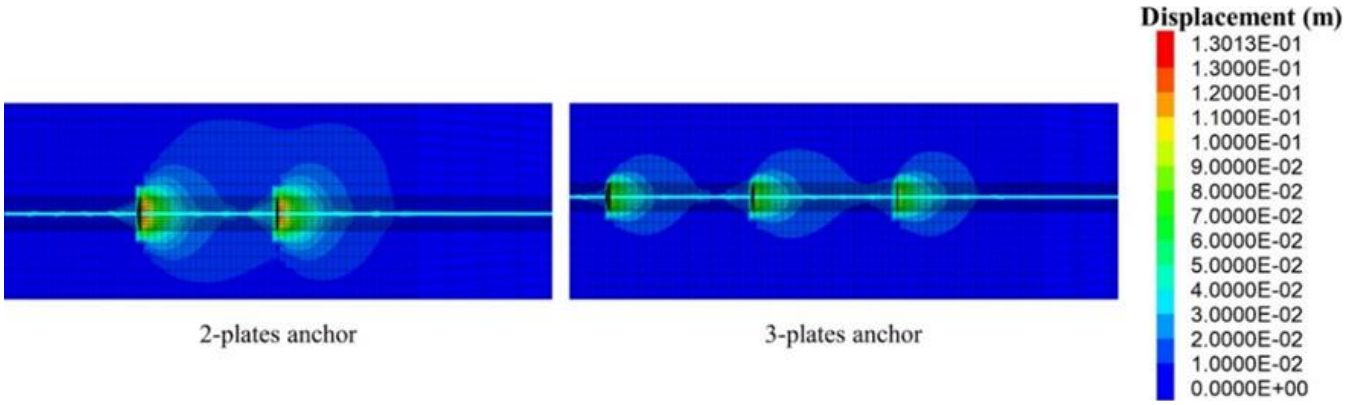

Fig. 6. Contour of the total displacement of the 2-plate and 3-plate reference models.

4- 1- Comparison with the analytical solution

As shown in Fig. 8, two types of failure mechanisms could occur for multi-plate anchors [23, 37, 41]: (1) Individual plate failure and (2) Cylindrical shear failure.

In the individual plate failure, each helical plate acts as a separate foundation. This failure mechanism occurs when the plate spacing is large enough. Considering helical plates as individual foundations, the analytical tensile capacity of multi-plate anchors is obtained from the below equation [37, 41]:

$$P_{u(1)} = \sum_{i=1}^{n} q_{ult} A_i + Q_{sh} \quad (1)$$

Where q_{ult} = ultimate bearing capacity of a helical plate, A = plate area (i.e., $A=\pi D^2/4$), Q_{sh} = skin resistance acting along the free length of the shaft, and n is the number of plates. According to Terzaghi's [42] solution, q_{ult} is computed from the following equation:

$$q_{ult} = 1.3cN_c + qN_q + 0.3\gamma DN_\gamma \quad (2)$$

Where N_c, N_q, and N_γ = bearing capacity factors, c = soil cohesion, q = surcharge stress at the given depth, γ = unit weight of the soil, and D is the diameter of the helical plate. The value of Q_{sh} is obtained from the below equation [37]:

$$Q_{sh} = (\sigma \tan\varphi + c)\ (4a)\ L \quad (3)$$

Where σ = the average vertical stress of the soil around the shaft, $4a$ = perimeter of the square shaft, and L is the free length of the shaft.

When the plates are close enough together, the failure zones formed in the vicinity of helical plates join each other. Therefore, helical plates could not act as individual foundations. In the cylindrical shear failure mechanism, it is assumed that the soil mass around plates is sheared as a cylindrical

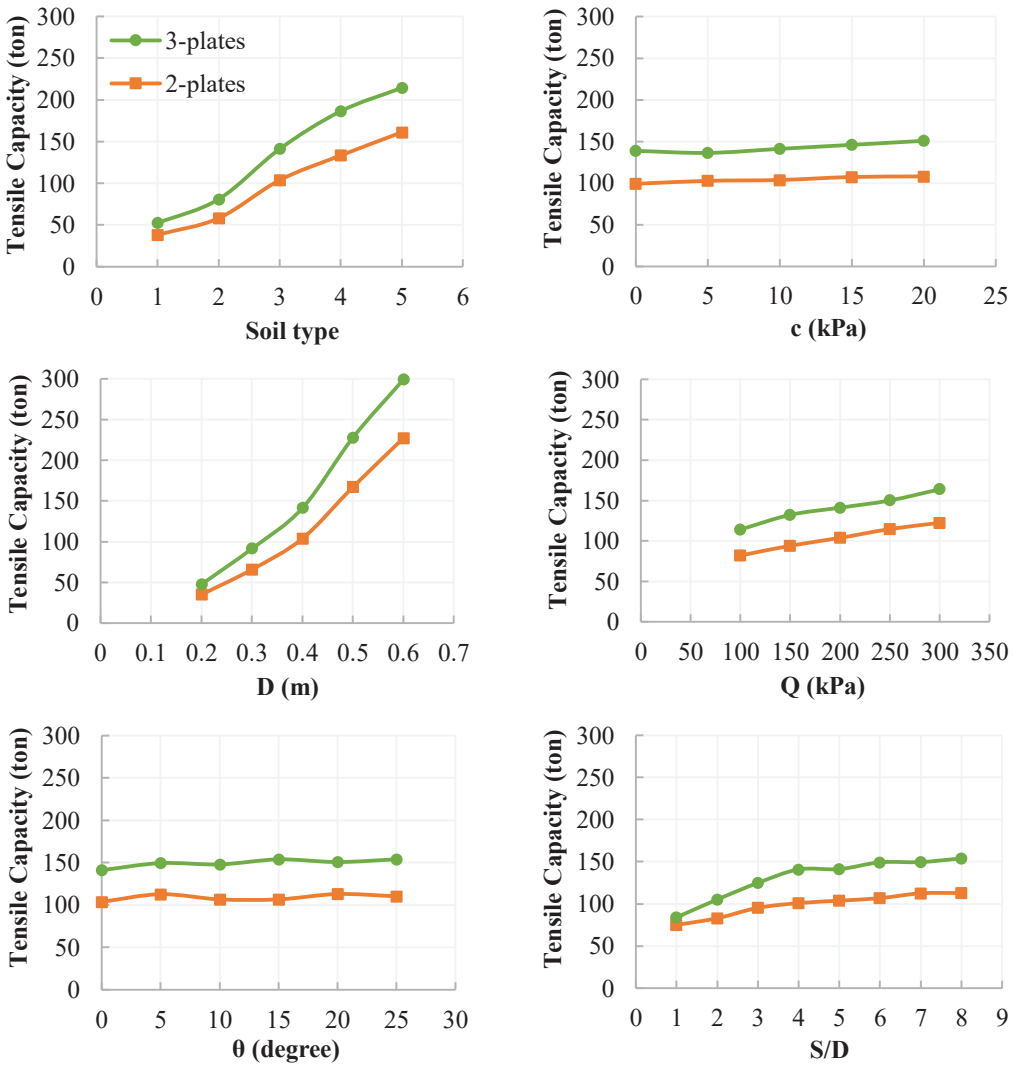

Fig. 7. Variation of the tensile capacities versus the soil type, surcharge, soil cohesion, plate diameter, plate spacing, and anchor inclination.

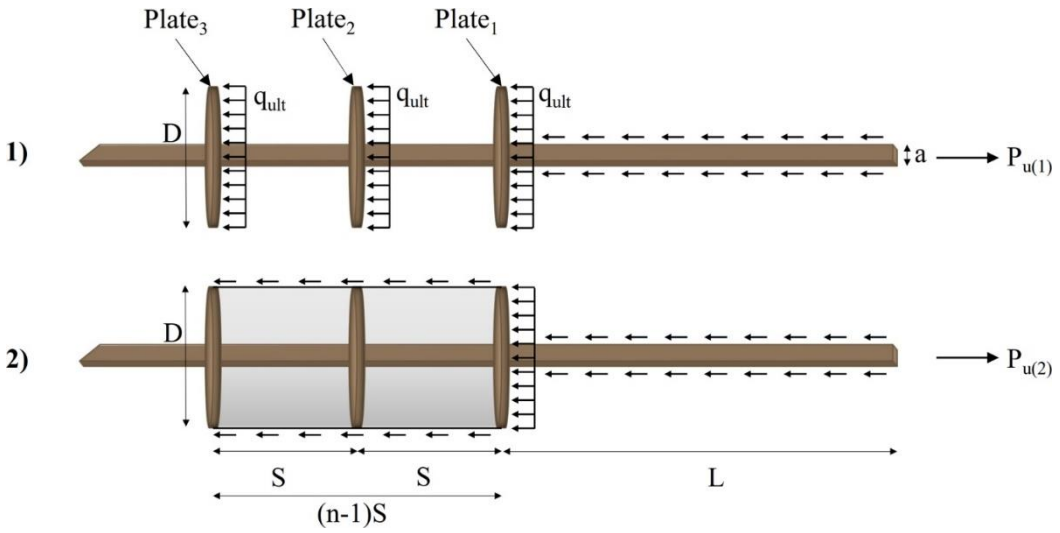

Fig. 8. Types of failure mechanism for multi-plate anchors: (1) Individual plate failure, and (2) Cylindrical shear failure.

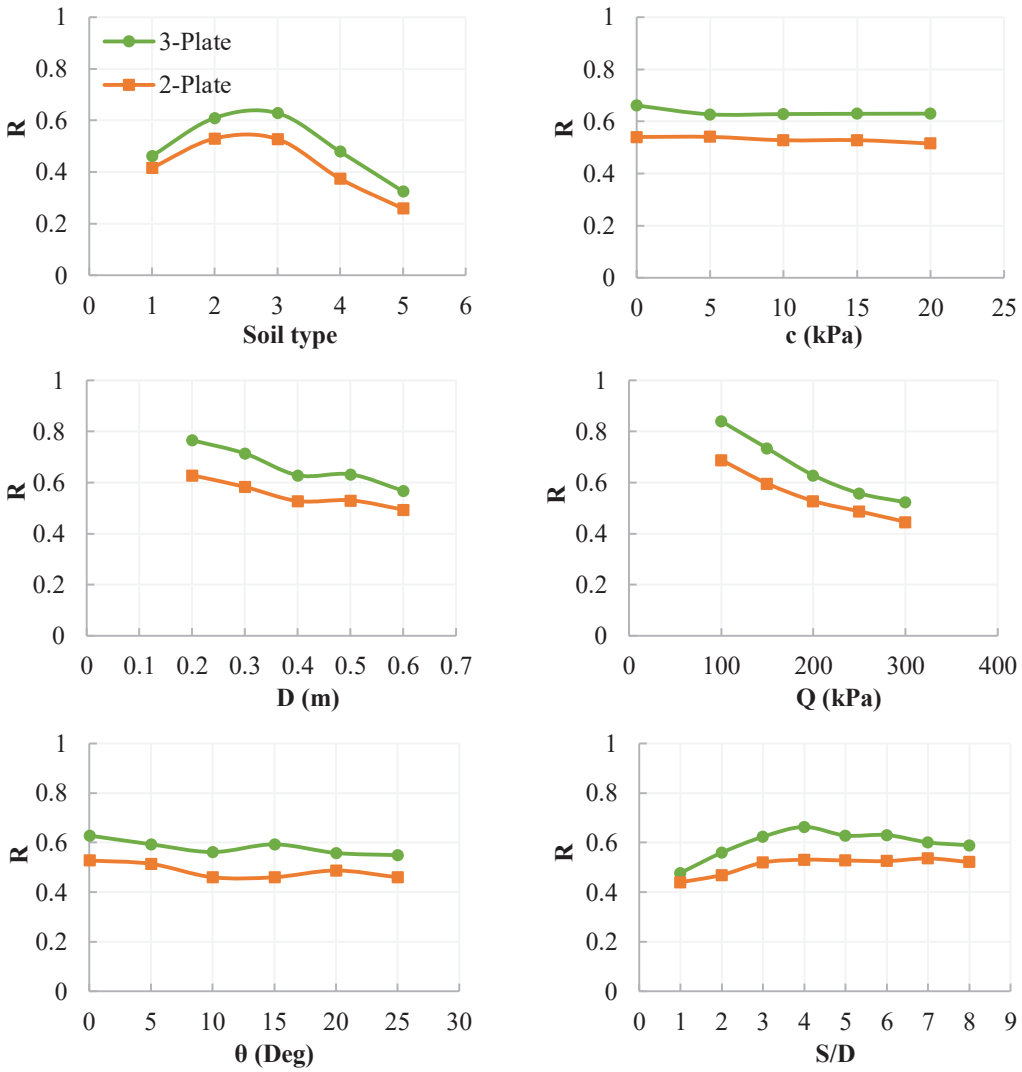

Fig. 9. Ratios of numerical to the analytical tensile capacity of the various models based on soil type, surcharge, soil cohesion, plate diameter, plate spacing, and anchor inclination.

block and moves along with plates. In this failure mechanism, the tensile capacity of helical anchors is computed from the sum of the load-bearing capacity of the first plate, skin resistances acting along the cylindrical block, and the free length of the shaft (Q_{sh}). Therefore, the ultimate tensile capacity of helical anchors in cylindrical shear mechanism is obtained from the below equation [37, 41]:

$$P_{u(2)} = q_{ult}\, A+(\sigma \tan\varphi+c)\,(n-1)S\,\pi D+Q_{sh} \quad (4)$$

Where σ = the average normal stress around the cylindrical block and (n-1) S is the length of the cylindrical block.

The analytical value of the tensile capacity for a helical anchor is considered as the minimum of $P_{u(1)}$ and $P_{u(2)}$ [37, 41].

Fig. 9 shows the ratios (R) of numerical to the analytical tensile capacity (i.e., P_u computed from the aforementioned equations) of various models. As can be seen, all R values are lower than one, generally ranging from about 0.25 to 0.85. The R values of 3-plates anchors are higher than those of 2-plates ones. Regarding the soil type, the R values increase from the loose to medium state and then decline to a very dense one. Moreover, it can be observed that the R values decrease by increasing the plate's diameter and surcharge. In addition, it can be considered that the R values stay almost unchanged by the increase of the soil cohesion and anchor inclination. As far as the plate spacing is concerned, it could be observed that the R values increase up to S/D=4 and then remain stationary.

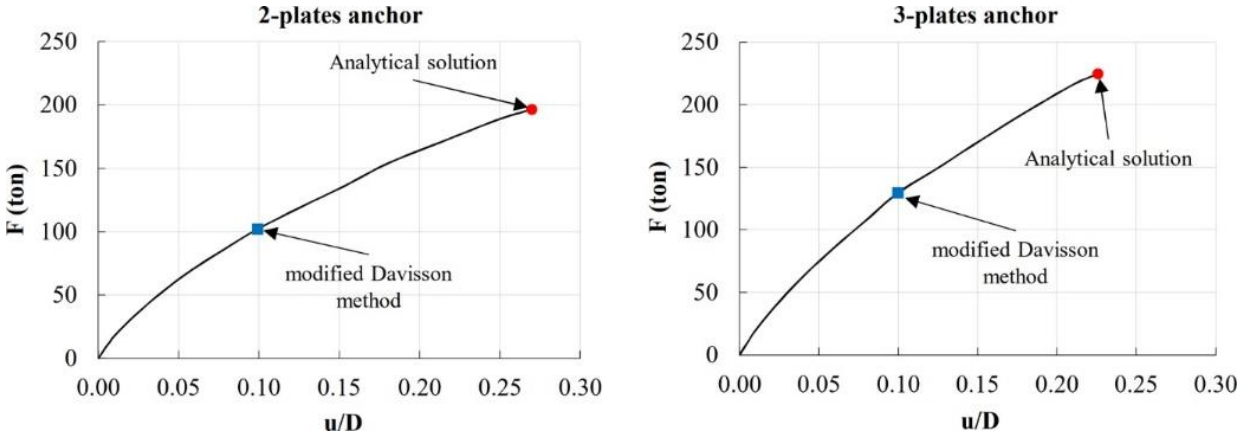

Fig. 10. Force-normalized net displacement curves of the reference models up to reaching the analytical tensile capacities.

The numerical to analytical tensile capacity ratios indicate that the modified Davisson criterion achieves lower tensile capacity compared with the analytical solution. This is because the net displacements required to mobilize the analytical values are higher than what is considered in the modified Davisson method (i.e., u/D = 0.10). For instance, Fig. 10 shows the force-normalized net displacement curves of the reference models up to reaching the analytical tensile capacities (197 and 225 tons for 2-plate and 3-plate anchors, respectively). The normalized net displacements at the analytical tensile capacities of 2-plates and 3-plates reference models are u/D = 0.27 and u = 0.23, respectively, which are about 2.5 times u/D = 0.10 in the modified Davisson method.

4- 2- Load-bearing shares of the helical plates and shaft

It is clear that in a multi-plate anchor, a share of the applied force (F) is sustained by the skin resistance along the shaft, and the remainder is tolerated by individual helical plates. F_s, F_{p1}, F_{p2}, and F_{p3} represent the shares of the shaft and 1st, 2nd, and 3rd plates, respectively. Figs. 11 and 12 compare the ratios of load-bearing shares of the shaft and helical plates to the total applied force (F_s/F, F_{p1}/F, F_{p2}/F, F_{p3}/F) at the end of loading (u/D = 0.10) for 2-plates and 3-plates models, respectively. Obviously, $F_{p1}/F+F_{p2}/F+F_s/F=1$ for 2-plates anchors and $F_{p1}/F+F_{p2}/F+F_{p3}/F+F_s/F=1$ for 3-plates anchors.

As can be seen, the 1st plate has the highest load-bearing shares, and the shaft has the lowest ones for all models. For 2-plate anchors, the load-bearing shares of the 1st and 2nd plates, as well as shaft, are on average 43, 37, and 20%, respectively. For 3-plate helical anchors, the load-bearing shares of the 1st, 2nd, and 3rd plates, as well as shaft, are on average 31, 27, 25, and 17%, respectively. From an engineering point of view, the load-bearing shares of the plates could be considered equal.

As can be seen in Figs. 11 and 12, the soil type and cohesion have little effect on the load-bearing shares of the shaft and helical plates. By increasing the surcharge, the load-bearing shares of the shaft increase slightly, and those of the helical plates decrease marginally. On the contrary, with the increase of the plate's diameter, the load-bearing shares of the shaft decrease, and those of the helical plates increase. By increasing S/D ratios, the load-bearing shares of the 1st plate decrease, and those of the shaft and other plates increase. This could be attributed to the transition of the failure mechanism that would be discussed in the next Section.

4- 3- Critical plates spacing

As explained previously in Section 4.1, two types of failure mechanisms may occur for helical multi-plate anchors: individual plate and cylindrical shear. The type of failure mechanism depends on the ratio of the spacing of the plates to diameter (i.e., S/D ratio). Individual plate failure occurs in the case of large S/D ratios, but the cylindrical shear takes place for small ones. In other words, by decreasing the S/D ratio, the type of failure mechanism changes from the individual plate to the cylindrical shear. The critical plate spacing is defined as the one about which the failure mechanism transition occurs. The corresponding S/D ratio is called the critical S/D ratio. As given in Table 4, the values ranging from 1 to 4 were previously reported for the critical S/D ratio.

In most of the previous numerical studies [27, 41, 43, 44], only displacement contours were used to determine the critical S/D ratio. However, the present study adopts a new method in which the variation of the load-bearing shares of the plates is taken into account, as well as displacement contours.

Fig. 13 illustrates the variations of the load-bearing share of each plate divided by the sum of the load-bearing shares of all plates (i.e., $F_{pi}/(\sum F_{pi})$) versus S/D for two and three-plate models. As can be seen, the curves become asymptotic for $S/D \geq 4$. This indicates that the load-bearing shares of the helical plates in the cases of $S/D \geq 4$ remain almost constant, which means that the plates act as individual foundations. In other words, the failure mechanism for $S/D \geq 4$ could be considered as the individual plate. However, for $S/D < 4$, the

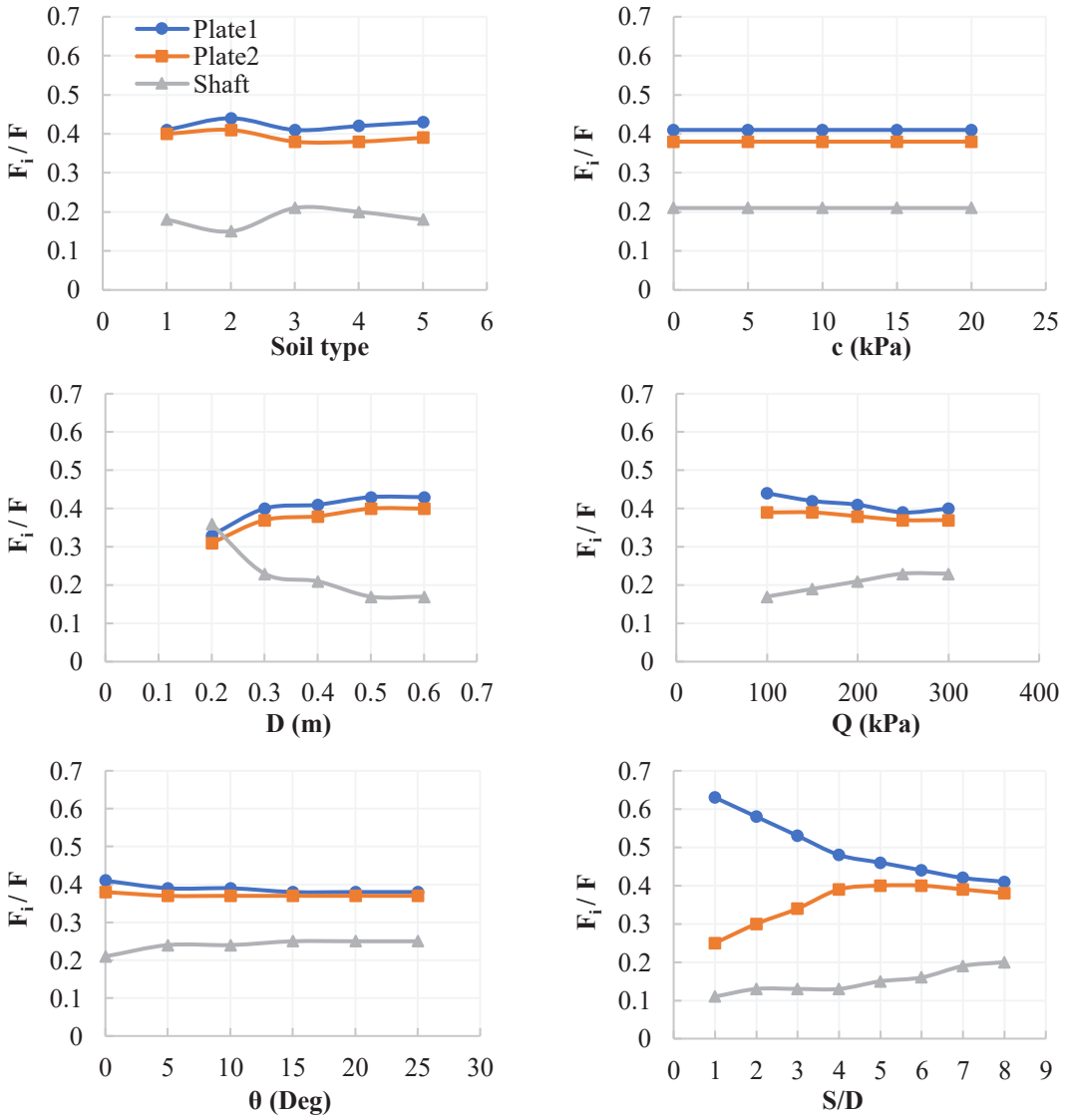

Fig. 11. Load-bearing shares of plates and shaft for 2-plate helical anchors based on soil type, surcharge, soil cohesion, plate diameter, anchor inclination, and plate spacing.

load-bearing share of the 1st plate is remarkably higher than other plates, decreasing with the increase of the *S*/*D* ratio. The contours of total displacement at the end of the test for 2-plate and 3-plate models with various *S*/*D* ratios are shown in Figs. 14 and 15, respectively. These contours confirm the aforementioned results. As can be seen, the failure zones formed around the helical plates are separate for $S/D \geq 4$ (individual plate failure). However, they are connected for $S/D<4$ (cylindrical shear failure). Therefore, $S/D = 4$ can be considered as the critical *S*/*D* ratio based on the results of the present paper, which is much closer to the one that was reported by Garakani and Maleki [21]. All of the contours in Figs. 14 and 15 show the variation of forces in helical plates and shafts and as can be seen in every contour the condition of the helical multi-plate anchor and its failure mode is completely governed by the value of *S*/*D*.

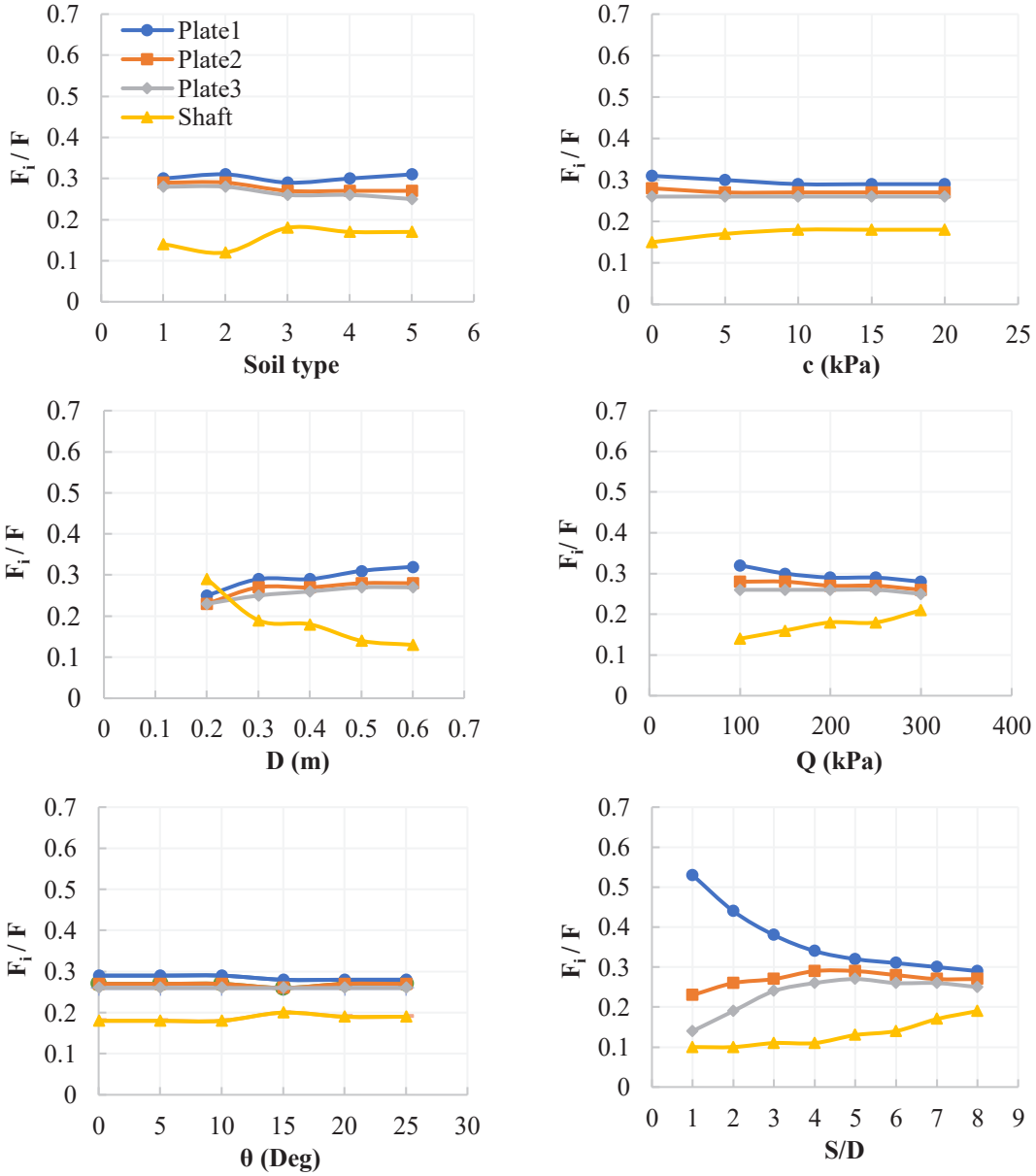

Fig. 12. Load-bearing shares of plates and shaft for 3-plate helical anchors based on soil type, surcharge, soil cohesion, plate diameter, anchor inclination, and plate spacing.

Table 4. Values for the critical S/D ratio reported in the literature.

Reference	Type of Study	Critical *S/D* ratio
Chance [37]	Numerical/Experimental	3
Merifield [43]	Numerical	1.58
Rawat and Gupta [27]	Numerical	3
Lutenegger [44]	Experimental	1.5
Rao, Prasad, and Shetty [45]	Experimental	1.5
Salhi, Nait-Rabah, Deyrat and Roos [14]	Numerical	1.5-2
Garakani and Maleki [21]	Numerical	3-4

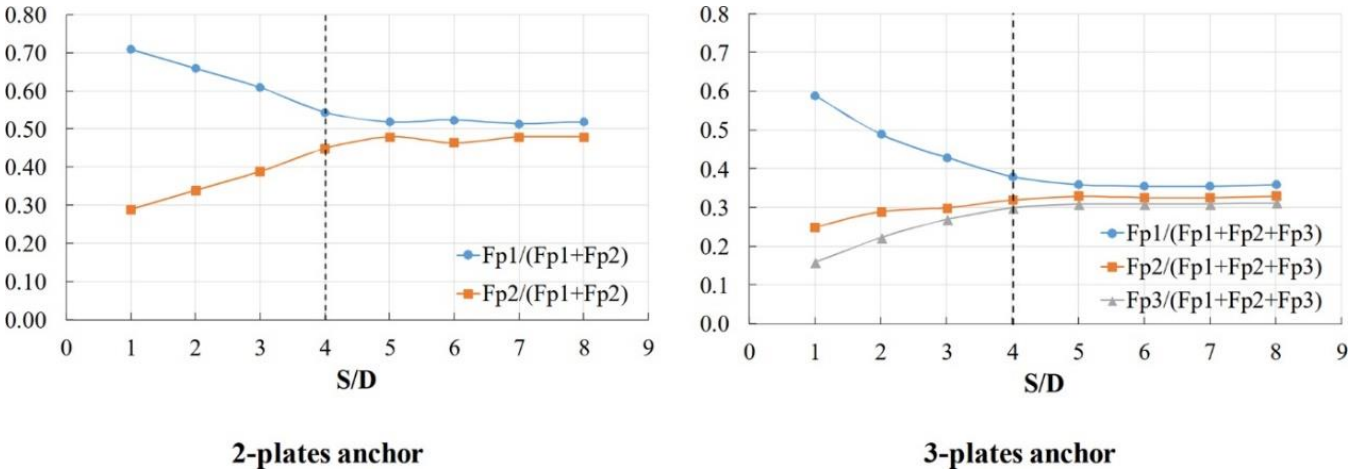

Fig. 13. Variations of Fpi/(∑Fpi) for the 2-plate and 3-plate helical anchor.

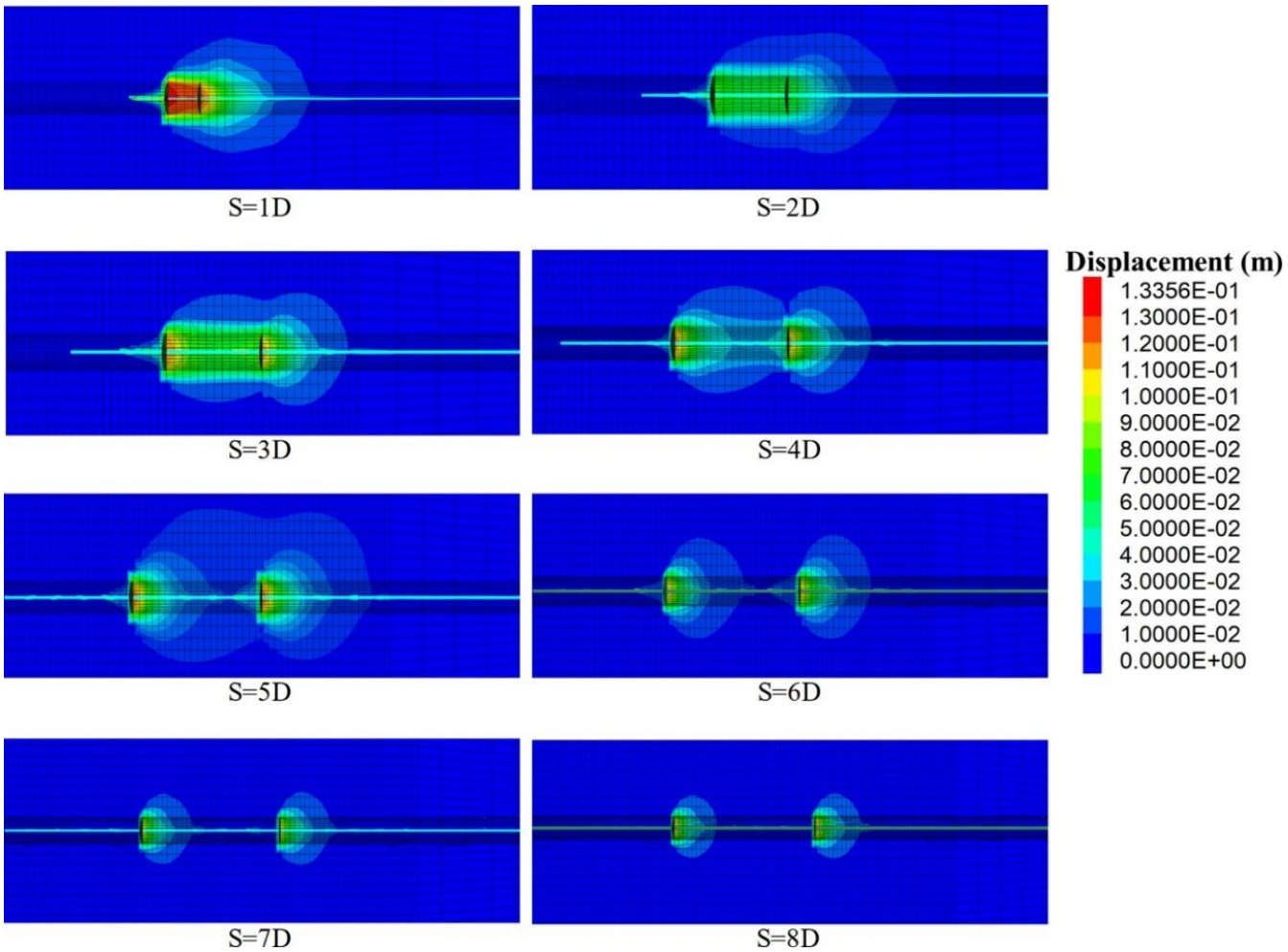

Fig. 14. Contours of total displacement at the end of the test for 2-plate models having various S/D ratios from S=1D to S=8D.

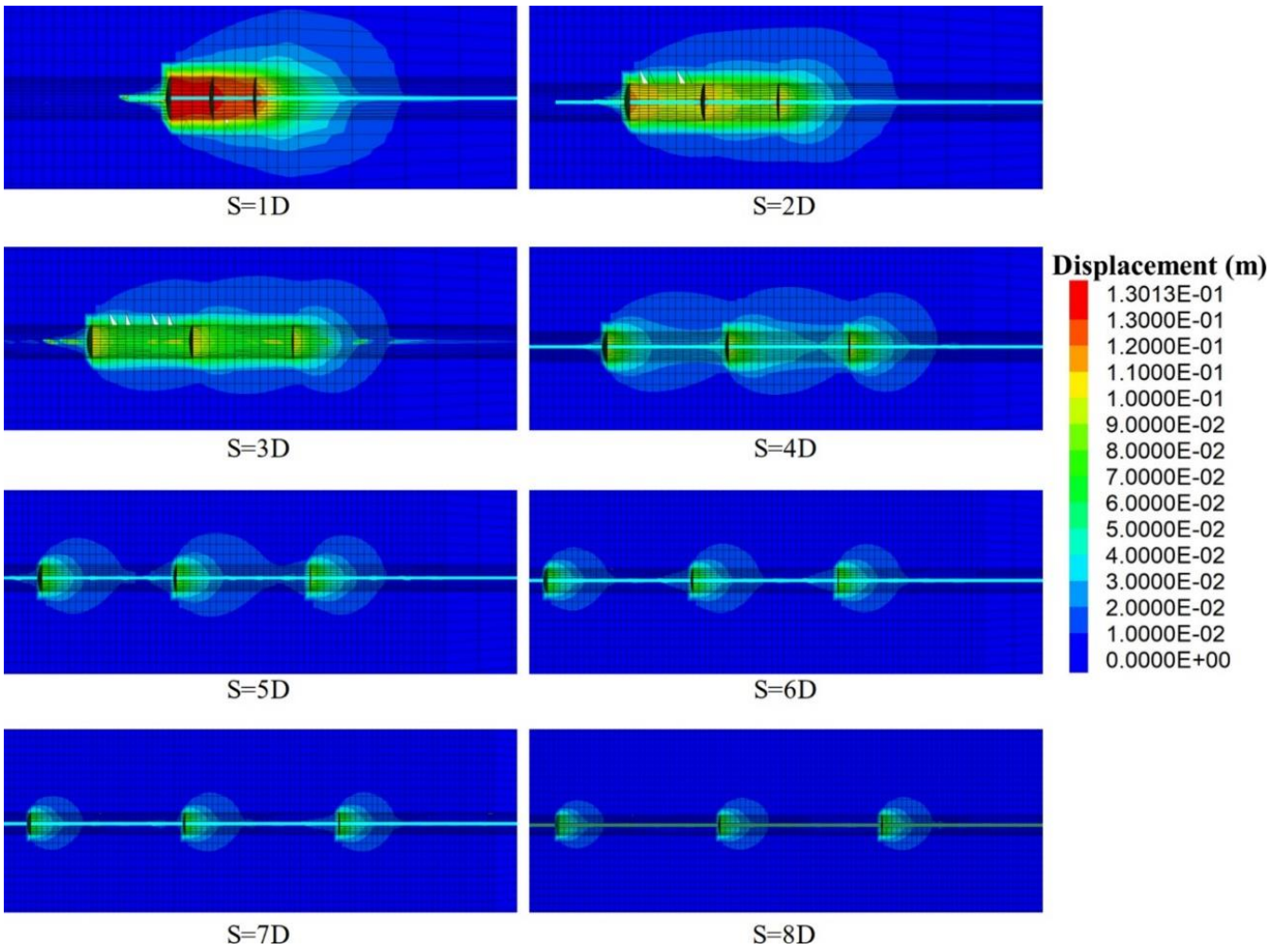

Fig. 15. Contours of total displacement at the end of the test for 3-plates models having various S/D ratios from S=1D to S=8D.

5- Conclusion

The present study employed a numerical modeling approach to investigate the tensile capacity of helical multi-plate anchors (2-plates and 3-plates anchors). The FLAC3D software was used for numerical simulations. For this purpose, first, a verification test based on an experimental study was performed to validate the adopted numerical modeling method. Then, a comprehensive parametric study was carried out by changing the soil type, soil cohesion, surcharge, plate diameter, plate spacing, and anchor inclination. In the present study, a new approach was selected for specifying the kind of failure mode in every helical multi-plate anchor. This new method relates to using the load-bearing share of every helical plate. The main results of the present paper are as follows:

- Increasing the soil relative density, plate diameter, and surcharge cause to increase in the tensile capacity of the helical anchors. However, the soil cohesion and anchor inclination have negligible effects on their tensile capacities.
- The ratios of numerical tensile capacities computed based on the modified Davisson criterion [4, 38-40] to analytical ones are less than one for all models. This indicates that the net displacements required to mobilize the analytical values of the tensile capacity are higher than those of the modified Davisson criterion.
- The load-bearing shares of the 1st and 2nd plates, as well as the shaft for 2-plates helical anchors, are on average 43, 37, and 20%, respectively. The load-bearing shares of the 1st, 2nd, and 3rd plates, as well as the shaft for 3-plates helical anchors, are on average 31, 27, 25, and 17%, respectively.
- The load-bearing shares of the shaft and plates remain almost unchanged by varying the soil cohesion and anchor inclination. However, decreasing the plate's diameter from 0.6 m to 0.2 m as well as increasing the surcharge from 100 kPa to 300 kPa cause to increase in the load-bearing shares of the shaft and reduce those of the plates which the value of these changes relates to parameters of helical multi-plate anchors and soil.
- By increasing the ratio of the plates spacing to diameter to 4 (i.e., S/D=4), the ratios of the load-bearing shares of the 1st plate to the sum of all plates (i.e., $F_{p1}/\sum F_p$) decrease while those of other plates increase. For $S/D \geq 4$, these ratios remain constant for all models. This indicates that the heli-

cal plates act as individual foundations for $S/D \geq 4$. In other words, the failure mechanism could be considered as the individual plate failure for the multi-plate anchors of $S/D \geq 4$ and cylindrical shear for those of $S/D < 4$. The union of failure zones formed at the vicinity of the plates in the displacement contours for models with $S/D < 4$ (see Figs. 14 and 15) confirms this conclusion. Therefore, the $S/D = 4$ could be considered the critical S/D ratio.

References

[1] R. Nazir, H.S. Chuan, H. Niroumand, K.A. Kassim, Performance of single vertical helical anchor embedded in dry sand, Measurement, 49 (2014) 42-51.

[2] S.P. Clemence, A.J. lutenegger, Industry survey of state of practice for helical piles and tiebacks, DFI., 9(1) (2015) 12-41.

[3] J. Beim, S.C. Luna, Results of dynamic and static load tests on helical piles in the varved clay of Massachusetts, DFI, 6(1) (2012) 58-67.

[4] [J.A. Cherry, H.A. Perko, Deflection of helical piles: a load tests database review, in: Proceedings of The 1st International Geotechnical Symposium on Helical Foundations, 2013.

[5] M. Elkasabgy, Dynamic and static performance of large-capacity Helical piles in cohesive soil, Ph.D. Thesis, The University of Western Ontario, Ontario, Canada, 2011.

[6] M. Elkasabgy, M.H. El Naggar, Dynamic response of vertically loaded helical and driven steel piles, Can. Geotech. J., 50(5) (2013) 521-535.

[7] S.-J. Feng, W.-D. Fu, H.-X. Chen, H.-X. Li, Y.-L. Xie, J. Li, Field tests of micro screw anchor piles under different loading conditions at three soil sites, Bull. Eng. Geol. Environ., 80(1) (2021) 127-144.

[8] A. Ghaly, A. Hanna, M. Hanna, Uplift behavior of screw anchors in sand. I: dry sand, J. Geotech. Eng. -ASCE, 117(5) (1991) 773-793.

[9] D. Hao, D. Wang, C.D. O'Loughlin, C. Guadin, Tensile monotonic capacity of helical anchors in sand: interaction between helices, Can. Geotech. J., 56(10) (2019) 1534-1543.

[10] A.A. Malik, J. Kuwano, S. Tachibana, T. Maejima, Effect of helix bending deflection on load settlement behavior of screw pile Acta Geotech., 14(5) (2019) 1527-1543.

[11] S. Mittal, S. Mukherjee, Behaviour of group of helical screw anchors under compressive loads, Geotech. Geol. Eng., 33(3) (2015) 575-592.

[12] H. Nagai, T. Tsuchiya, M. Shimada, Influence of installation method on performance of screwed pile and evaluation of pulling resistance, Soils Found., 58(2) (2018) 355-369.

[13] Z.A. Perez, J.A. Sciavon, Numerical and experimental study on influence of installation effects on behavior of helical anchors in very dense sand, Can. Geotech. J., 55(8) (2018) 1067-1080.

[14] L. Salhi, O. Nait-Rabah, C. Deyrat, C. Roos, Numerical modeling of single helical pile behavior under compressive loading in sand, EJGE, 18 (2013) 4319-4338.

[15] J.A. Schiavon, C.d.H.C. Tsuha, L. Thorel, Monotonic, cyclic and post-cyclic performances of single-helix anchor in residual soil of sandstone J. Rock Mech. Geotech. Eng., 11(4) (2019) 824-836.

[16] G. Spagnoli, C. de Hollanda Cavalanti Tusha, A review on the behavior of helical piles as a potential offshore foundation system, Mar. Geores. Geotechnol., 38(9) (2020) 1-24.

[17] H. Tokhi, G. Ren, J. Li, Laboratory study of a new screw nail and its interaction in sand, Comput. Geotech., 78 (2016) 144-154.

[18] H. Tokhi, G. Ren, J. Li, Laboratory pullout resistance of a new screw soil nail in residual soil, Can. Geotech. J., 55(5) (2018) 609-619.

[19] D. Wang, R. Merifield, C. Gaudin, Uplift behavior of helical anchors in clay, Can. Geotech. J., 50(6) (2013) 575-584.

[20] B. Cerfontaine, J.A. Knappett, M.J. Brown, A. Bradshaw, Effect of soil deformability on the failure mechanism of shallow plate or screw anchors in sand, Comput. Geotech, 109 (2019) 34-45.

[21] A.A. Garakani, J. Maleki, Load capacity of Helical Piles with different geometrical aspects sandy and clayey soils: A Numerical Study, in: International Congress and Exhibition Sustainable Civil Infrastructures, Springer, Egypt, 2019, pp. 73-84.

[22] P. Ghosh, S. Samal, Interaction effect of helical anchors in cohesive soil using finite element analysis, Geotech. Geol. Eng., 35(4) (2017) 1475-1490.

[23] O. Kwon, J. Lee, G. Kim, I. Kim, J. Lee, Investigation of pullout load capacity for helical anchors subjected to inclined loading conditions using coupled Eulerian-Lagrangian analyses, Comput. Geotech, 111 (2019) 66-75.

[24] R. Merifield, C. Smith, The Ultimate Uplift Capacity of Multi-Plate Anchor in Undrained Clay, in: Soil behaviour and geo-micromechanics, 2010, pp. 74-79.

[25] A. Pandey, V.B. Chauhan, Numerical analysis for the evaluation of pull-out capacity of helical anchors in sand, in: International Congress and Exhibition Sustainable Civil Infrastructures, 2019, pp. 207-218.

[26] S. Rawat, A. Gupta, Analysis of a nailed soil slope using limit equilibrium and finite element methods, Int. J. Geosynth. Ground Eng., 2(4) (2016) 1-23.

[27] S. Rawat, A.K. Gupta, Numerical modeling of pullout of helical soil nail, J. Rock Mech. Geotech. Eng., 9(4) (2017) 648-658.

[28] A. Sharma, S. Guner, System-level modeling methodology for capturing the pile cap, helical pile group, and soil interaction under uplift loads, Eng. Struct., 220 (2020).

[29] G. Spagnoli, S. Mendez, M. Carlos, C. de Hollanda Cavalanti Tusha, P. Oreste, Parametric analysis for the estimation of the installation power for large helical piles in dry cohesionless soils, Int. J. Geotech. Eng., 14(5) (2020) 569-579.

[30] C. Tang, K.-K. Phoon, Model uncertainty of cylindrical

shear method for calculating the uplift capacity of helical anchors in clay, Eng. Geol., 207 (2016) 14-23.

[31] D. Wang, Y. Hu, M. Randolph, Three-dimensional large deformation finite element analysis of plate anchors in uniform clay, J. Geotech. Geoenviron. Eng., 136(2) (2010) 355-365.

[32] H.M. Bak, A.M. Halabian, H. Hashemolhosseini, M. Rowshanzamir, Axial response and material efficiency of tapered helical piles, J. Rock Mech. Geotech. Eng., 13(1) (2021) 176-187.

[33] S. Rawat, A. Gupta, A. Kumar, Pullout of soil nail with circular discs: a three-dimensional finite element analysis, J. Rock Mech. Geotech. Eng., 9(5) (2017) 967-980.

[34] Y.U. Sharif, M.J. Brown, B. Cerfontaine, C. Davidson, M.O. Ciantia, J.A. Knappett, J.D. Ball, A. Brennan, C. Augarde, W. Coombs, A. Blake, D. Richards, D. White, M. Huisman, M. Ottolini, Effects of screw pile installation on installation requirements and in-service performance using the discrete element method, Canadian Geotechnical Journal, 58(9) (2021) 1334-1350.

[35] B. Cerfontaine, M. Ciantia, M.J. Brown, Y.U. Sharif, DEM study of particle scale and penetration rate on the installation mechanisms of screw piles in sand, Computers and Geotechnics, 139 (2021) 17.

[36] Itasca Consulting Group, FLAC3D 6.0 User Manual, 2017.

[37] Chance, Chance Technical Design Manual, 4th ed., Chance Company, USA, 2004.

[38] G. Abdelrahman, E. Shaarawi, K. Abouzaid, Interpretation of axial pile load test results for continuous flight auger piles, in: Emerging Technologies in Structural Engineering. Proceedings of the 9th Arab Structural Engineering Conference 2003, pp. 796.

[39] F. Baligh, G. Abdelrahman, Modification of Davisson's method, in: Proceedings of the 16th International Conference on Soil Mechanics and Geotechnical Engineering, 2005, pp. 2079-2082.

[40] L.D.C. Garcia, Assessment of Helical Anchors Bearing Capacity For Offshore Aquaculture Applications, The University of Maine, 2019.

[41] A.A. Garakani, A Guideline For Design, Execution And Testing of Energy Piles, NRI, Iran, 2019.

[42] K. Terzaghi, Theoretical Soil Mechanics, New York, (1943) 11-15.

[43] R. Merifield, Ultimate uplift capacity of multiplate helical type anchors in clay, J. Geotech. Geoenviron. Eng., 137(7) (2011) 704-716.

[44] A.J. Lutenegger, Behavior of multi-helix screw anchors in sand, in: Proceedings of the 14th Pan-American Conference on Soil Mechanics and Geotechnical Engineering, Toronto, Ontario, 2011.

[45] S.N. Rao, Y. Prasad, M.D. Shetty, The behavior of model screw piles in cohesive soils, Soils Found., 31(2) (1991) 35-50.

HOW TO CITE THIS ARTICLE

M.Hazeghian , M. Abdoli, A. R. Javid, Three-Dimensional Numerical Study of the Tensile Capacity of Helical Multi-Plates Anchors , AUT J. Civil Eng., 6(1) (2022) 119-132.

DOI: 10.22060/ajce.2022.20915.5785